1521-0111/96/3/401–407$35.00
MOLECULAR PHARMACOLOGY

https://doi.org/10.1124/mol.119.116475
Mol Pharmacol 96:401–407, September 2019

Dantrolene Requires Mg^{2+} and ATP To Inhibit the Ryanodine Receptor

Gyula Diszházi,[1] Zsuzsanna Édua Magyar,[1] János András Mótyán, László Csernoch, István Jóna, Péter Pál Nánási, and János Almássy

Departments of Physiology (G.D., Z.É.M., L.C., P.P.N., J.A.) and Biochemistry and Molecular Biology (J.A.M.), and Research Centre for Molecular Medicine (I.J.), Faculty of Medicine, and Department of Dental Physiology and Pharmacology, Faculty of Dentistry (P.P.N.), University of Debrecen, Debrecen, Hungary

Received February 25, 2019; accepted July 7, 2019

ABSTRACT

Dantrolene is a ryanodine receptor (RyR) inhibitor, which is used to relax muscles in malignant hyperthermia syndrome. Although dantrolene binds to the RyR protein, its mechanism of action is unknown, mainly because of the controversial results showing that dantrolene inhibited Ca^{2+} release from intact fibers and sarcoplasmic reticulum (SR) vesicles, but failed to inhibit single RyR channel currents in bilayers. Accordingly, it was concluded that an important factor for dantrolene's action was lost during the purification procedure of RyR. Recently, Mg^{2+} was demonstrated to be the essential factor for dantrolene to inhibit Ca^{2+} release in skinned muscle fibers. The aim of the present study was to confirm these results in Ca^{2+} release and bilayer experiments, using SR vesicles and solubilized channels, respectively. Our Ca^{2+} release experiments demonstrated that the effect of dantrolene and Mg^{2+} was cooperative and that ATP enhanced the inhibiting effect of dantrolene. Namely, 10 μM dantrolene reduced RyR channel open probability by ~50% in the presence of 3 mM free Mg^{2+} and 1 mM ATP, whereas channel activity further decreased to ~20% of control when [ATP] was increased to 2 mM. Our data provide important complementary information that supports the direct, Mg^{2+}-dependent mechanism of dantrolene's action and suggests that dantrolene also requires ATP to inhibit RyR.

Introduction

Skeletal muscle contraction is caused by the rapid increase of myoplasmic Ca^{2+}. Under physiologic conditions, this Ca^{2+} signal is generated by the action potential that triggers Ca^{2+} release from the sarcoplasmic reticulum (SR) by opening ryanodine receptor (RyR)–Ca^{2+} channels in the SR membrane. However, under certain pathologic conditions, such as malignant hyperthermia (MH) syndrome, Ca^{2+} release may develop in unexcited muscle. MH is an idiosyncratic reaction of susceptible individuals to volatile anesthetics, like halothane, isoflurane, or enflurane. These patients carry certain point mutations in the RyR1 gene, which sensitize the channel to be activated by volatile anesthetics. Therefore, even therapeutic concentrations of these anesthetics cause muscle contracture in the patients. Increased muscle activity during the MH episode leads to hyperthermia, acidosis, and hyperkalemia and finally to death—unless immediate interventions are taken, including cooling the whole body and resolving the muscle rigidity with the RyR-inhibitor dantrolene (e.g., Fruen et al., 1997; Zucchi and Ronca-Testoni, 1997; Fill and Copello, 2002). Because appropriate dantrolene treatment fails to rescue 5% of MH patients, improving its therapeutic efficiency is an important challenge, which cannot be completed without identifying the ideal conditions for drug action. This identification process was set back by the lack of our knowledge about dantrolene's mechanism of action, which primarily arises from controversial data, reported by our group as well as by others (Szentesi et al., 2001; Diaz-Sylvester et al., 2008; Wagner et al., 2014). Particularly, our group demonstrated that the drug inhibited Ca^{2+} release from intact fibers and SR vesicles, but failed to inhibit single RyR channel currents (Szentesi et al., 2001). We then concluded that an important factor for dantrolene's action was lost during the purification procedure of RyR. Thus, in spite of the fact that dantrolene is the only muscle relaxant used to treat MH episodes and its binding site was identified in the primary sequence of the RyR protein (Paul-Pletzer et al., 2002, 2005), its exact mechanism of action is still unknown. Apparently, to discover the mechanism of dantrolene's action, we must identify the missing factor(s) required for RyR inhibition.

The present work was motivated by two recent studies, which aimed to identify these unknown ingredients. In the

This work was supported by the Hungarian National Research Development and Innovation Office (PD112199 to J.A. and K115397 to P.P.N.). J.A. is supported by the Lajos Szodoray Scholarship of the University of Debrecen and the János Bolyai scholarship of the Hungarian Academy of Sciences. This work was also supported by Projects GINOP-2.3.2–15-2016-00040 and EFOP-3.6.2-16-2017-00006 (to L.C., J.A., and P.P.N.), which are cofinanced by the European Union and the European Regional Development Fund.
[1]G.D.and Z.É.M. contributed equally to this work.
https://doi.org/10.1124/mol.119.116475.
S This article has supplemental material available at molpharm.aspetjournals.org.

ABBREVIATIONS: 4CMC, 4-chloro-m-cresol; aa, amino acid; APIII, antipyrylazo III; CAM, calmodulin; CHAPS, 3-[(3-cholamidopropyl) dimethylammonio]-1-propanesulfonic acid; DBS, dantrolene binding site; MH, malignant hyperthermia; NsoI, N-terminal solenoid; P_o, open probability; RyR, ryanodine receptor; SR, sarcoplasmic reticulum; TC, terminal cisternae.

more recent paper, Choi et al. (2017) postulated that only Mg^{2+} was absent in single-channel experiments; thus, they investigated whether Mg^{2+} was required for dantrolene's effect. They tested dantrolene in the presence of different Mg^{2+} concentrations in skinned muscle fibers and found that 10 μM dantrolene required at least 1 mM Mg^{2+} to significantly inhibit Ca^{2+} release. These authors did not provide single-channel current data to confirm their result; direct evidence proving that the action of dantrolene is mediated by Mg^{2+} through a direct allosteric mechanism on the RyR1 protein itself is still missing. Therefore, the present work aims to examine purified (accessory protein-free) RyR1s to demonstrate that the channel requires the direct binding of Mg^{2+} to become dantrolene-sensitive.

The other paper identified calmodulin (CaM) as the essential factor for the effect of dantrolene (Oo et al., 2015), whose role in the drug action was further investigated in the present work.

Materials and Methods

Animals. All experiments complied with the Hungarian Animal Welfare Act, the 2010/63/EU guideline of the European Union, and had the approval of the Animal Welfare Committee of the University of Debrecen (22/2012/DEMÁB). Rabbits (~4 kg body weight, 6- to 10-month-old males, $n = 4$; Juráskó, Debrecen-Józsa, Hungary) were killed by using a guillotine. Musculus longissimus dorsi was dissected and frozen in 50 g aliquots. Using these aliquots, terminal cisternae vesicles were prepared three times, and RyR channels were purified five times.

Terminal Cisternae Vesicle Preparation and RyR Purification. SR terminal cisternae (TC) were isolated from rabbit skeletal muscle with differential centrifugation. RyR was purified from TC vesicles by solubilization in 1% 3-[(3-cholamidopropyl)dimethylammonio]-1-propanesulfonic acid (CHAPS) and 0.45% phosphatidylcholine and 1 mM dithiothreithol, as described previously (Szentesi et al., 2001; Geyer et al., 2015; Sárközi et al., 2017).

Solubilized RyRs were purified on linear sucrose gradient (10%–28% sucrose, 0.08%–0.65% CHAPS, 0.005 g/ml phosphatidylcholine, 786 μM NaCl, 80 μM EGTA, 118 μM $CaCl_2$, 3.93 mM AMP $\times$ $6H_2O$, 15.7 mM, and 510 μM dithiothreithol Na-1,4-piperazinediethanesulfonic acid, pH 7.3) at 100,000*g* overnight. RyR-containing fractions of the gradient were collected, and 50 μl aliquots were snap-frozen.

Ca^{2+} Release Assay. TC vesicles (100 μg) were dispersed in 2 ml imaging medium containing 92.5 mM KCl, 1 or 3 mM $MgCl_2$, 0.5 or 1.5 mM ATP, 7.5 mM Na-piro-phosphate, 18.5 mM 4-morpholinepropanesulfonic acid, and 250 μM antipyrylazo III (APIII), pH 7.0. The vesicles were actively loaded in the cuvette with Ca^{2+} using Sarco-Endoplasmic Reticulum Ca^{2+}-ATP-ase (SERCA)activity by the addition of 4 $\times$ 10 μl 5 mM $CaCl_2$. The extravesicular Ca^{2+} was monitored by the transmittance of the Ca^{2+} indicator APIII using a spectro-fluorimeter at 710 nm. Ca^{2+} release was triggered using 400 μM 4-chloro-*m*-cresol (4CMC) in the presence or absence of 10 μM dantrolene at different Mg^{2+} and ATP concentrations (Sárközi et al., 2007).

The rate of Ca^{2+} release was obtained by measuring the slope of the initial segment of the process. Values were normalized to the average of the first five data points. The time between the Ca^{2+} release curves was assessed at the half-maximum points.

RyR1 Reconstitution and Single-Channel Current Recording in Planar Lipid Bilayers. Measurements of channel activity were carried out using purified RyRs incorporated into planar lipid bilayers. Bilayers were painted using a mixture of phospholipids (phosphatidylethanolminine, phosphatidylserine, and phosphatidylcholine 5:4:1, >50 mg/ml, dissolved in decan) across a 200 μM diameter aperture of a Delrin cap in a symmetrical buffer solution containing 250 mM K^+ as a charge carrier and 50 μM free Ca^{2+}. RyR channels were incorporated to bilayers by dispersing 50 μl purified RyR suspension in 1 ml recording solution. Dantrolene was applied to the cytoplasmic side of RyR under different conditions: 50 μM free Ca^{2+}, 3.94 mM total Mg^{2+}, and 1 mM ATP (= 3 mM free Mg^{2+}) or, alternatively, 500 nM free Ca^{2+} and 2 mM ATP in the cytoplasmic compartment. Further experiments were performed with 100 nM free Ca^{2+}, 1 mM ATP, and 100 nM CaM. The channel current was recorded using an Axopatch 200 amplifier and pCLAMP 6 software at a membrane potential of $\pm$60 mV. Currents were filtered at 1 kHz through an eight-pole low-pass Bessel filter and digitized at 3 kHz (Sárközi et al., 2017). After 30-second stirring, drug action was recorded at least for 5 minutes, and longer than 3-minute segments were analyzed.

Western Blot Analysis. Whole-muscle homogenate, SR microsome suspension, and purified RyR1 samples (identical to the samples used in the functional experiments) were loaded onto 7.5% SDS-polyacrylamide gel. After electrophoresis, the proteins were transferred onto nitrocellulose membrane (1620115; Bio-Rad) at 100 V for 60 minutes. The membrane was blocked by 2.5% dry milk in Tris-buffered saline (pH 7.5) at room temperature for 1 hour, followed by incubation with a mouse anti-calmodulin monoclonal primary antibody (ab5494-200; Abcam) in a 1:800 dilution. The membrane was incubated with the primary antibody at 4°C for 16 hours. After washing the membrane with Tris-buffered saline complemented with Tween 20, it was incubated at room temperature for 1 hour with anti-mouse IgG secondary antibody (A4416; Sigma-Aldrich) in 1:5000 dilution. To detect proteins on the membrane, SuperSignal West Pico chemiluminescent substrate has been used (Thermo Fisher Scientific). Both primary and secondary antibodies were diluted in Tris-buffered saline complemented with Tween 20 containing 0.1% dry milk.

Statistical Analysis. Data are presented as the average of at least three independent experiments (n, number of experiments). Averages are expressed as mean $\pm$ S.D. value.

Sample size had been adapted after initial results have been obtained.

Molecular Modeling. Coordinate files have been downloaded from Protein Data Bank, and we used PyMOL Molecular Graphics System (Version 1.3; Schrödinger) for structural alignment and to prepare structural figures. The relative positions of N-terminal solenoid (NSol) (590–609) and junctional solenoid (1656–1672) helices were determined by the alignment of the following structures: PDBIDs: 5T9M, 5T15, 5T9V, 5TAX, 5TAS, and 5TB1.

Results

First, Ca^{2+} release experiments were performed using heavy SR vesicles, which correspond to the terminal cisternae of the intact SR. Accordingly, these vesicles contained both RyRs and SERCA pumps, which offers the option to load them with Ca^{2+} actively, using the SERCA pump. To this end, vesicles were suspended in imaging medium, and were loaded with four subsequent aliquots of Ca^{2+} (indicated by asterisks in Fig. 1) in the presence of 1 mM Mg^{2+} and 0.5 mM ATP. These Mg^{2+} and ATP concentrations were minimal requirements for proper loading.

The extravesicular Ca^{2+} level was monitored by measuring the transmittance of the imaging buffer at 710 nm, in which decrease in APIII transmittance signal represents an increase in extravesicular Ca^{2+}. After finishing the loading procedure, the transmittance of the solution stayed constant, because during this time the basic vesicular Ca^{2+} leak was balanced by Ca^{2+} uptake.

The first series of experiments were designed to test whether Mg^{2+} affects the dantrolene action on Ca^{2+} release. The effect of dantrolene was tested on the parameters of agonist-induced Ca^{2+} release in 1 or 3 mM Mg^{2+} (Fig. 1A). The Ca^{2+} release was triggered 1 minute after reaching the steady-state transmittance

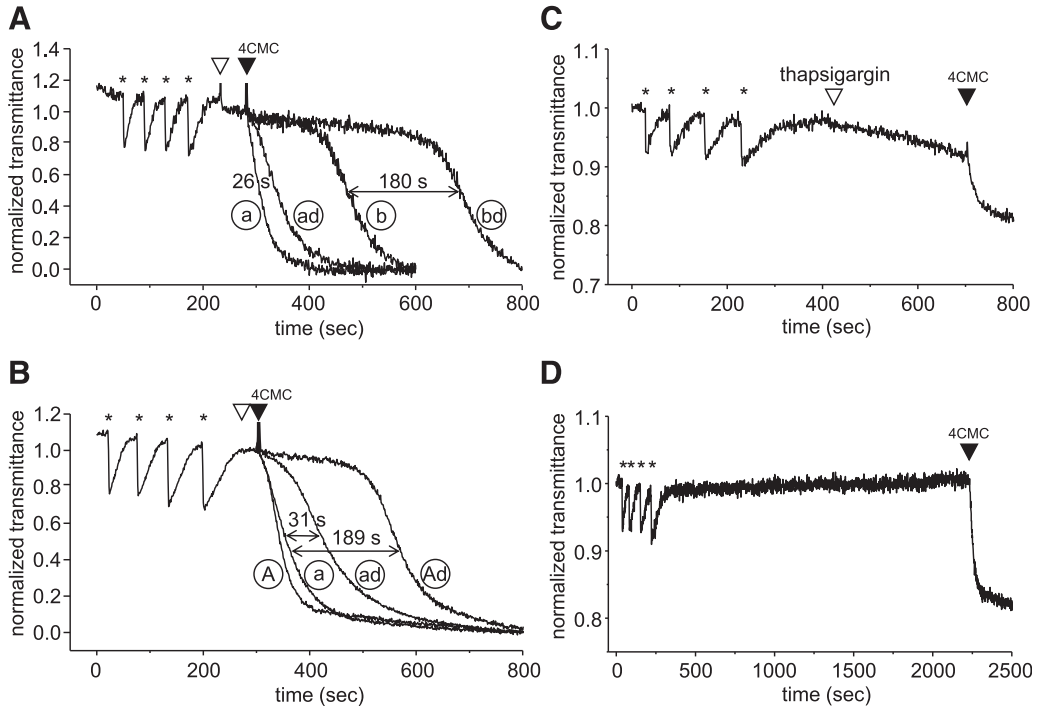

Fig. 1. Dantrolene delays the onset of agonist-induced Ca^{2+} release from SR vesicles. Extravesicular Ca^{2+} level was monitored using APIII. SR vesicles were loaded with four subsequent aliquots of Ca^{2+} using SERCA activity. Injections of Ca^{2+} are labeled with asterisks (*). (A) Ca^{2+} release was triggered using 4CMC in 1 or 3 mM Mg^{2+} under control conditions (curves "a" and "b") or in the presence of 10 μM dantrolene (curves "ad" and "bd") (n = 3 to 4). (B) Ca^{2+} release curves recorded in 0.5 or 1.5 mM ATP in the absence (curves "a" and "A," respectively) or presence of dantrolene (curves "ad" and "Ad"). Addition of dantrolene or DMSO is labeled with white and the addition of 4CMC with black arrowheads. (C) Spontaneous Ca^{2+} leak from SR vesicles after thapsigargin-treatment. (D) Transmittance-curve of untreated vesicles in the presence of 1 mM Mg^{2+} and 0.5 mM ATP. At the end of measurements shown in panels C and D, Ca^{2+} release was elicited using 4CMC to verify the functional integrity of the vesicles.

by using 400 μM 4CMC (black arrowhead) in the presence or absence of dantrolene (white arrowhead). We found that in 1 mM Mg^{2+}, 4CMC caused a robust Ca^{2+} release immediately, whereas both 3 mM Mg^{2+} and dantrolene induced a significant delay in the Ca^{2+} release curves (156 and 26 seconds; see the delays in Fig. 1A between records indicated as "a" and "ad" and "a" and "b," respectively). The rate of Ca^{2+} release was significantly lower in the presence of three compared with 1 mM Mg^{2+} (2.04 $\pm$ 0.08 vs. 0.9 $\pm$ 0.07 nmol Ca^{2+}/s, n = 3 and 4), whereas dantrolene only slightly decreased the rate of release (2.04 $\pm$ 0.08 vs. 1.4 $\pm$ 0.22 nmol Ca^{2+}/s in 1 mM Mg^{2+}, while 0.9 $\pm$ 0.07 vs. 0.73 $\pm$ 0.03 nmol Ca^{2+}/s in 3 mM Mg^{2+}).

Nevertheless, dantrolene caused an additional 180-second delay in 3 mM Mg^{2+} (Fig. 1A, curves "b" and "bd," horizontal arrow), indicating that the suppressive effects of dantrolene and Mg^{2+} were synergistically potentiating (consistent with Choi et al., 2017).

The characteristic action of the drug, that is, causing a delay in the onset of Ca^{2+} release, raised the hypothesis that when ATP was present in the imaging medium, the drug was able to prevent Ca^{2+} release, but after SERCA-consumed ATP and [ATP] fell below a certain level, dantrolene lost its effectivity (in spite of the fact that the RyR inhibitor Mg^{2+} accumulated during this process and Mg^{2+} failed to prevent Ca^{2+} release). This result indicates the essential role of ATP in the effect of dantrolene. Therefore, we tested the drug with a higher [ATP] of 1.5 mM and found that the delay in Ca^{2+} release was longer by 158 seconds than observed under control conditions in the presence of 0.5 mM ATP (31 seconds between "a" and "ad" curves vs. the 189-second difference found between curves "a" and "Ad" in Fig. 1B), whereas 1.5 mM ATP alone did not cause any delay (Fig. 1B). These results confirm the hypothesis that ATP is also required for the inhibiting effect of dantrolene.

An alternative reason to possibly account for the dantrolene-induced delay would be a significant background Ca^{2+} leak from the vesicles because, if the background leak through RyR was significant, balancing it by Ca^{2+} uptake through SERCA would consume an elevated amount of ATP. Therefore, inhibiting this resting leak with dantrolene would preserve ATP for SERCA function, which would fuel SERCA for a longer period to prevent the triggered Ca^{2+} release, that is, when the solution runs below the threshold [ATP] later. However, our result that increased [ATP] alone did not cause any delay in the onset of Ca^{2+} release suggests that the ATP-dependent delay in the presence of dantrolene is not a secondary, SERCA-mediated mechanism. To rule out this alternative possibility, we determined the resting leak of our vesicles. To this end, vesicles were loaded with Ca^{2+} as before in 0.5 mM ATP, and 20 μM thapsigargin (SERCA pump inhibitor) was added to the buffer, which induced a slow spontaneous Ca^{2+} release (Fig. 1C). In a different set of experiments, loaded vesicles were left untreated and were allowed to run free (Fig. 1D). In this case, no Ca^{2+} release was observed for periods longer than 25 minutes, suggesting that SERCA was able to compensate the basal Ca^{2+} leak so the medium did not run out of ATP during this time. This result implies that our medium did not consume significant amounts of ATP, whereas the loaded vesicles were incubated with dantrolene (for 60 seconds). These data rejected our alternative hypothesis that ATP saved by dantrolene would be responsible

for the delay, and justify the idea that the effect of dantrolene on the RyR allosterically relies on ATP.

Similar experiments (in 0.5 mM ATP and 1 mM Mg^{2+}) were performed using cardiac vesicles, but we failed to reproduce these results (Supplemental Fig. 1).

As dantrolene was previously shown to be ineffective in bilayer studies (Szentesi et al., 2001), the most important question of our study was whether Mg^{2+} is the magic ingredient for the action of dantrolene. Therefore, we tested whether Mg^{2+} was able to endow solubilized skeletal muscle-type RyRs with dantrolene sensitivity in bilayer studies. Representative records are shown in Fig. 2A. The channel was incorporated into the bilayer in 50 μM Ca^{2+} (control), and a few minutes later 3 mM Mg^{2+} was added to the cytoplasmic side of the same channel, which significantly suppressed the open probability (P_o) of the channel. Thereafter, 1 mM ATP was included in the same compartment of the bilayer chamber, which increased the activity of the RyR. After reaching steady state, 10 μM dantrolene was added to the recording medium. Our single-channel analysis demonstrated that dantrolene decreased the P_o of the Mg^{2+}–ATP-treated channels by 48% ± 5% (P_o = 0.0177 ± 0.025 vs. 0.0123 ± 0.021, n = 12, effect size: −0.23; 95% confidence interval: −1.03; 0.58). The average change of P_o (±S.D.) obtained in 12 individual RyR is shown in Fig. 2C (third symbol). In four cases [ATP] was raised further from 1 to 2 mM after dantrolene treatment. Surprisingly, the P_o further decreased—instead of being increased by ATP—to 17% ± 8% of control (0.0177 ± 0.025 vs. 0.0018 ± 0.003, n = 4, effect size: −0.71; 95% confidence interval: −1.83; 0.48) (Fig. 2C, fourth symbol), which is in accordance with the therapeutic effects of the drug. These results also indicate that ATP enhances the effect of dantrolene. However, when Mg^{2+} was omitted from the recording medium, dantrolene remained ineffective in the presence of 2 mM ATP (91% ± 3% of control, P_o = 0.38 ± 0.35 vs. 0.35 ± 033, n = 10, effect size: −0.08; confidence interval: −0.96; 0.8) (Fig. 2C, second symbol), suggesting that ATP is a necessary, but not an exclusive requirement for RyR to be inhibited by dantrolene.

Dantrolene was also proposed to require CaM to inhibit single-channel activity (Oo et al., 2015). However, the SR microsome fraction is very unlikely to retain its CaM content during differential centrifugation; the results by Oo et al. (2015) raise the assumption that SR microsomes, which were sensitive to dantrolene in the Ca^{2+} release experiments, contained CaM. Therefore, Western blot analysis was performed to test whether our SR microsomes and purified RyR suspension contained CaM. In Fig. 3A, a Western blot is displayed, showing that neither the SR microsome fraction

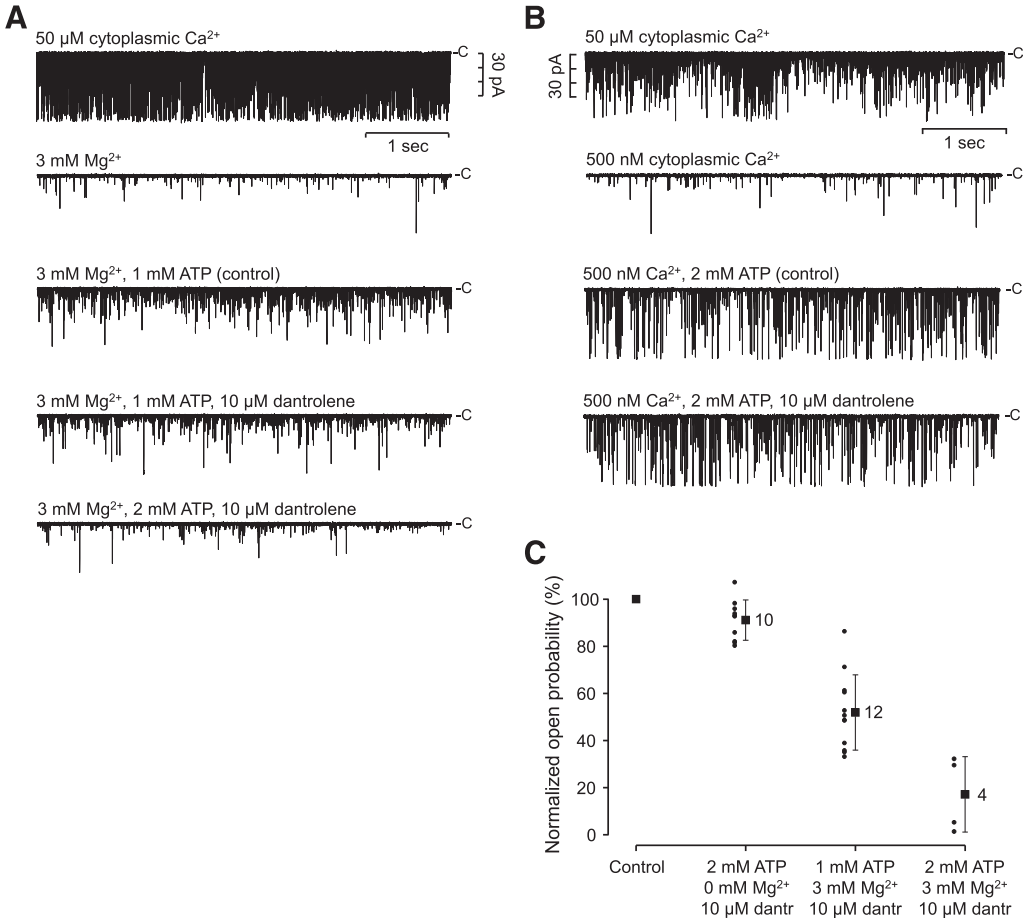

Fig. 2. Dantrolene suppresses RyR P_o in lipid bilayers. (A and B) Single-channel currents of RyR1. Openings of the channel correspond to downward deflections. Representative current traces of a single channel under control conditions (50 μM Ca^{2+}), after the addition of 1 mM Mg^{2+} and 0.5 mM ATP, are shown, respectively. Bottom trace: channel current in the presence of 1 mM Mg^{2+}, 0.5 mM ATP, and 10 μM dantrolene. Average P_o are shown above the representative current curves. Quantitative data are presented in (C). Data are expressed as mean ± S.D. Individual data points are represented by small dots.

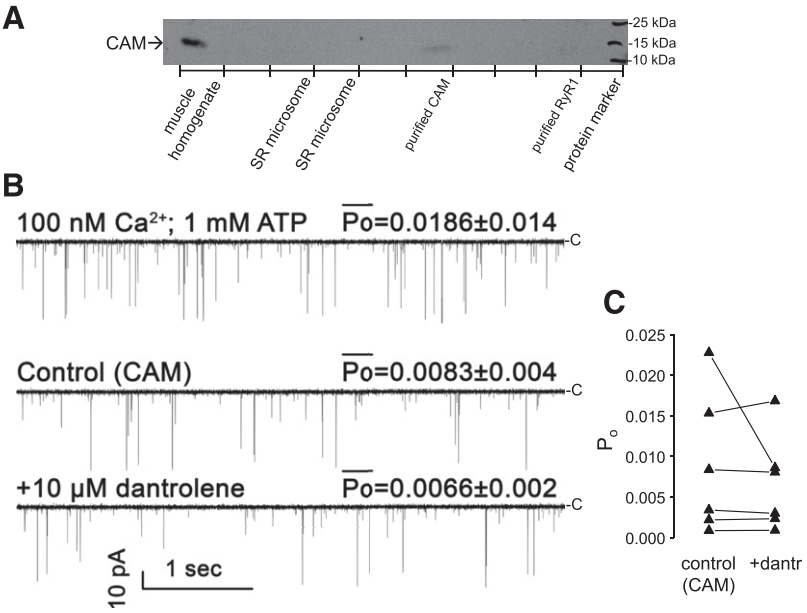

Fig. 3. Dantrolene remained ineffective in the presence of calmodulin. (A) Western blot analysis of CaM in SR microsomes and a purified RyR sample. Whole-cell homogenate and purified CaM served as positive control. (B) Single-channel currents recorded in 100 nM Ca^{2+}, 1 mM ATP, and 100 nM CaM under control conditions (top traces) and during dantrolene treatment (bottom trace). (C) P_o values of six individual channels under control conditions and during dantrolene treatment.

nor the purified RyR1 suspension contained detectable amounts of CaM. In contrast, we were able to identify CaM in whole-cell homogenate and purified CaM samples, as indicated by the bands of the corresponding lanes around the 15-kDa protein marker. Although the fact that SR vesicles lack CaM, but dantrolene inhibited Ca^{2+} release from these vesicles, does not support the idea that CaM is required for the action of dantrolene, we further tested the action of dantrolene in single-channel experiments in the presence of 100 nM CaM. Five-second–long segments of such current records are shown in Fig. 3B under control conditions (100 nM Ca^{2+}, 1 mM ATP, 100 nM CaM) and during dantrolene treatment. P_o of six individual RyR1 channels is displayed in the graph of Fig. 3C, showing that dantrolene failed to inhibit RyR1 in the presence of CaM under our experimental conditions.

Discussion

The motivation of the current research was to resolve the discrepancy that dantrolene inhibited Ca^{2+} release from intact fibers, but failed to inhibit Ca^{2+} release channels in bilayer studies. Our work was directly stimulated by the recent publication by Choi et al. (2017), demonstrating that Mg^{2+} is an essential cofactor for the dantrolene effect in skinned muscle fibers. Indeed, as Mg^{2+} inhibits channel activity and thus renders the evaluation of further RyR inhibition problematic, Mg^{2+} was omitted from all the single-channel studies that investigated the action of dantrolene, including Cherednichenko et al. (2008) (Szentesi et al., 2001). They performed experiments in a medium containing 100 nM Ca^{2+} and 1 mM ATP plus 1 μM CaM and showed that dantrolene did not inhibit RyR1. However, to date, the only study that demonstrated the suppressive effect of dantrolene on RyR in bilayers was published by Oo et al. (2015), who showed that CaM was required for dantrolene to inhibit both skeletal muscle (RyR1), and cardiac RyRs (RyR2), although their recording medium did not contain Mg^{2+}. As our data and the data by Choi et al. (2017) were different, new questions arose about the molecular mechanism of the dantrolene action. The solution for the discrepancy between these conflicting results may again be related to the composition of the recording medium. In contrast to standard recording buffers, Oo et al. (2015) buffered their solution to the redox potential of ~−200 mV using glutathione, providing a reducing environment to the proteins, which may account for their observations.

Another possible reason for the conflicting results is that purification of RyRs with CHAPS may alter how dantrolene works.

In this study, we aimed to add important complementary single-channel information to research by Choi et al. (2017) and used similar conditions in our bilayer chamber to those found to be essential for the action of dantrolene in the Ca^{2+} release assay (i.e., 3 mM Mg^{2+} and 1 mM ATP). As expected, under these conditions, dantrolene significantly inhibited the P_o of the channels. Most importantly, our data demonstrate for the first time that dantrolene requires the direct binding of Mg^{2+} to RyR, but not to other accessory proteins—as we used CHAPS-solubilized, naked RyRs.

Furthermore, we have shown that P_o was reduced by dantrolene in the presence of higher [ATP] (2 mM), strongly suggesting that ATP potentiates the effect of dantrolene. It should be noted that these single-channel data tightly correlate with our Ca^{2+} release results.

Our finding that ATP is also required for the drug action is particularly important, because it modifies the message of the paper by Choi et al. (2017). The commentaries by Choi et al. (2017) and (Cannon, 2017) propose that diminishing [ATP] and consequent elevation of the free [Mg^{2+}] during MH episodes is what may be needed for achieving the efficacy of dantrolene in the presence of halothane, whereas our data suggest that dantrolene would lose efficacy at severely low [ATP] even at otherwise sufficiently high [Mg^{2+}]. This means that there might be an optimal time window during the MH episode for dantrolene application and also highlights the importance of the immediate treatment (i.e., before [ATP] falls below the critical threshold level) (Choi et al., 2017).

The Putative Dantrolene Binding Site. Photoaffinity-labeling studies identified the dantrolene binding site (DBS)

in the NSol domain, in the helix formed by the amino acids (aa) in the 590–609 position (Paul-Pletzer et al., 2002). Later, experiments using domain–peptide probe approach suggested that this region (called DP1) and another one, named DP4 (aa 2442–2477), are critically important to form domain–switch interactions and may interact with one another (Kobayashi et al., 2005). According to the most widely accepted model, the zipped configuration of the interdomain interactions formed by the N-terminal (aa 35–614) and central domains (aa 2129–2458) is transmitted toward the pore to mediate the closed conformation of the channel. Stimulation of RyR unzips these molecular switches and causes the opening of the pore. Similarly, MH mutations in the N-terminal disease hotspot may directly unzip and destabilize these interfaces, which results in overreactive channels. Dantrolene would fix these imperfections by pinching out the loosened structure at a certain point (around aa 590–609) and restabilizes the overall structure by an allosteric mechanism (Ikemoto and Yamamoto 2002; Yamamoto and Ikemoto 2002; Kobayashi et al., 2004, 2005; Tung et al., 2010).

To understand the relationships of the DP1 domain (DBS), we visualized this domain in a three-dimensional structure of the rabbit RyR1 and explored the putative interaction surfaces in the proximity of DP1 (Efremov et al., 2015; Yan et al., 2015; Zalk et al., 2015; des Georges et al., 2016). It is clearly visible that DP1 and DP4 are located far away from the Ca^{2+} (Mg^{2+}), ATP, and caffeine binding sites. DP1 is located in the Nsol, and DP4 is in the bridging solenoid domain, and these two subdomains do not interact with each other. However, our detailed analysis revealed several interdomain interactions in DP1's neighborhood. DP1 aligns with a helix in junctional solenoid (aa 1657–1678) (Fig. 4B, circled), and its N-terminal loop gets in close contact with a loop in bridging solenoid domain, formed by the aa 2166–2171 (Fig. 4B, dotted circle). Apparently, these interdomain interfaces form an important keystone of this region of the structure. This hypothesis is in line with the fact that these sequences are highly conserved among species, and, in addition, they contain four well-known MH mutation sites (R614, R2163, V2168, T2206). Mutations at these points may influence the affinity of dantrolene to its binding site, which may account for the ineffectiveness of dantrolene in some cases. Furthermore, the C-terminal end of DP1 potentially interacts with SPRY3 sequences (aa 1591–1595) too (Fig. 4B, dashed circle).

Our experimental data suggest two possible molecular mechanisms for the action of dantrolene: 1) dantrolene binding requires a specific allosterically modified state, which is mediated by Mg^{2+} and ATP, or alternatively, 2) dantrolene binding allosterically increases the affinity of RyR to Mg^{2+} (as proposed by Choi et al., 2017). Our in silico analysis supports the latter possibility because relative interdomain distances are similar in the structures determined in the presence of caffeine, ATP, and Ca^{2+} (open state, 5TAQ.pdb) or in the conformational state induced by EGTA (closed state, 5TB1.pdb), respectively (des Georges et al., 2016). This structural information indicates that the DBS is not subject to structural realignments during gating; therefore, it is most probably always accessible—no matter whether Mg^{2+} occupies the Ca^{2+} binding sites—indicating that dantrolene most probably acts by allosterically increasing the affinity of Mg^{2+} to RyR.

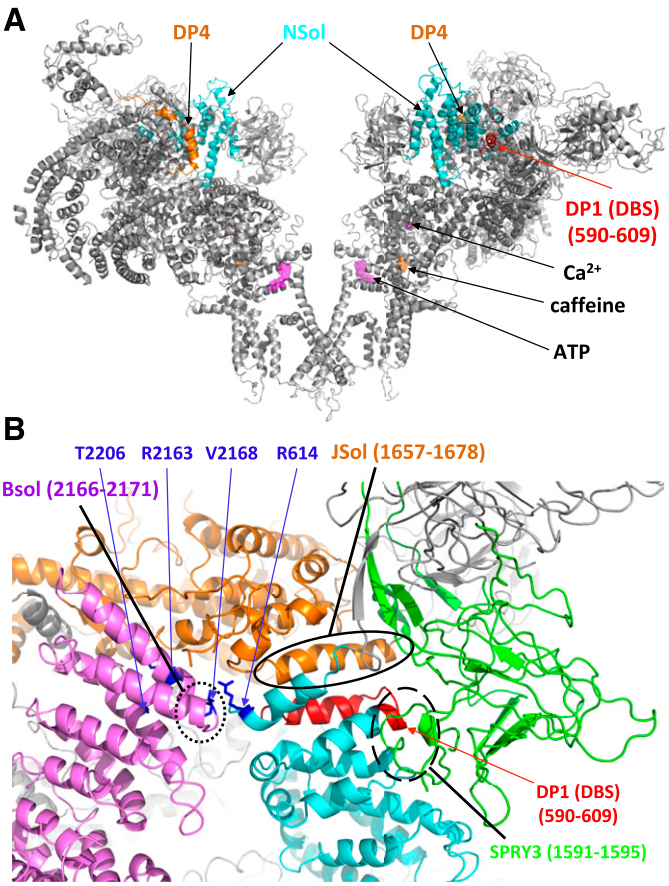

Fig. 4. Representation of the putative DBS and its interdomain interactions in the 3D structure of RyR1. (A) Two subunits (caffeine/ATP/Ca^{2+} dataset, 5TAQ.pdb) of RyR1 are shown by cartoon representation (side view). ATP, Ca^{2+}, and caffeine are shown by sphere representation and are colored by magenta and orange, respectively. NSol domain (393–627) is shown by cyan. The DBS (590–609) is highlighted by red. The DP4 region (2442–2477) is shown by orange. Sequence is numbered according to the rabbit Ryr1. (B) Shows the putative interaction surfaces in the proximity of the DBS. The NSol domain (393–627) is highlighted by cyan, the SP1a/RyR domain 3 (SPRY3) domain (1242–1656) by green, the junctional solenoid (JSol) domain (1657–2144) by orange, and the bridging solenoid (BSol) domain (2145–3613) by violet. DBS (590–609) is highlighted by red. Regions of neighboring domains located in the proximity of DBS are circled. Hydrogen bonds are formed between aa N1678-Q618, G1677-R615, D1658-H597; Q2169-A613; and D591-R1594, D591-R1594, L590-R1594. Well-known mutation sites around the DBS are shown by blue sticks and are indicated by blue numbers and arrows. R614 of human Ryr1 corresponds to R615 in rabbit Ryr1. See text for further details.

Authorship Contributions

Participated in research design: Almássy.

Conducted experiments: Diszházi, Magyar, Mótyán, Almássy.

Contributed new reagents or analytic tools: Finana, Cathala.

Performed data analysis: Diszházi, Magyar, Mótyán, Csernoch, Jóna, Nánási, Almássy.

Wrote or contributed to the writing of the manuscript: Diszházi, Magyar, Mótyán, Csernoch, Jóna, Nánási, Almássy.

References

Cannon SC (2017) Mind the magnesium, in dantrolene suppression of malignant hyperthermia. *Proc Natl Acad Sci USA* **114**:4576–4578.

Cherednichenko G, Ward CW, Feng W, Cabrales E, Michaelson L, Samso M, López JR, Allen PD, and Pessah IN (2008) Enhanced excitation-coupled calcium entry in myotubes expressing malignant hyperthermia mutation R163C is attenuated by dantrolene. *Mol Pharmacol* **73**:1203–1212.

Choi RH, Koenig X, and Launikonis BS (2017) Dantrolene requires Mg^{2+} to arrest malignant hyperthermia. *Proc Natl Acad Sci USA* **114**:4811–4815.

des Georges A, Clarke OB, Zalk R, Yuan Q, Condon KJ, Grassucci RA, Hendrickson WA, Marks AR, and Frank J (2016) Structural basis for gating and activation of RyR1. *Cell* **167**:145–157.e17.

Diaz-Sylvester PL, Porta M, and Copello JA (2008) Halothane modulation of skeletal muscle ryanodine receptors: dependence on Ca^{2+}, Mg^{2+}, and ATP. *Am J Physiol Cell Physiol* **294**:C1103–C1112.

Efremov RG, Leitner A, Aebersold R, and Raunser S (2015) Architecture and conformational switch mechanism of the ryanodine receptor. *Nature* **517**:39–43.

Fill M and Copello JA (2002) Ryanodine receptor calcium release channels. *Physiol Rev* **82**:893–922.

Fruen BR, Mickelson JR, and Louis CF (1997) Dantrolene inhibition of sarcoplasmic reticulum Ca^{2+} release by direct and specific action at skeletal muscle ryanodine receptors. *J Biol Chem* **272**:26965–26971.

Geyer N, Diszházi G, Csernoch L, Jóna I, and Almássy J (2015) Bile acids activate ryanodine receptors in pancreatic acinar cells via a direct allosteric mechanism. *Cell Calcium* **58**:160–170.

Ikemoto N and Yamamoto T (2002) Regulation of calcium release by interdomain interaction within ryanodine receptors. *Front Biosci* **7**:d671–d683.

Kobayashi S, Bannister ML, Gangopadhyay JP, Hamada T, Parness J, and Ikemoto N (2005) Dantrolene stabilizes domain interactions within the ryanodine receptor. *J Biol Chem* **280**:6580–6587.

Kobayashi S, Yamamoto T, Parness J, and Ikemoto N (2004) Antibody probe study of Ca^{2+} channel regulation by interdomain interaction within the ryanodine receptor. *Biochem J* **380**:561–569.

Oo YW, Gomez-Hurtado N, Walweel K, van Helden DF, Imtiaz MS, Knollmann BC, and Laver DR (2015) Essential role of calmodulin in RyR inhibition by dantrolene. *Mol Pharmacol* **88**:57–63.

Paul-Pletzer K, Yamamoto T, Bhat MB, Ma J, Ikemoto N, Jimenez LS, Morimoto H, Williams PG, and Parness J (2002) Identification of a dantrolene-binding sequence on the skeletal muscle ryanodine receptor. *J Biol Chem* **277**:34918–34923.

Paul-Pletzer K, Yamamoto T, Ikemoto N, Jimenez LS, Morimoto H, Williams PG, Ma J, and Parness J (2005) Probing a putative dantrolene-binding site on the cardiac ryanodine receptor. *Biochem J* **387**:905–909.

Sárközi S, Almássy J, Lukács B, Dobrosi N, Nagy G, and Jóna I (2007) Effect of natural phenol derivatives on skeletal type sarcoplasmic reticulum Ca^{2+} -ATPase and ryanodine receptor. *J Muscle Res Cell Motil* **28**:167–174.

Sárközi S, Komáromi I, Jóna I, and Almássy J (2017) Lanthanides report calcium sensor in the vestibule of ryanodine receptor. *Biophys J* **112**:2127–2137.

Szentesi P, Collet C, Sárközi S, Szegedi C, Jona I, Jacquemond V, Kovács L, and Csernoch L (2001) Effects of dantrolene on steps of excitation-contraction coupling in mammalian skeletal muscle fibers. *J Gen Physiol* **118**:355–375.

Tung CC, Lobo PA, Kimlicka L, and Van Petegem F (2010) The amino-terminal disease hotspot of ryanodine receptors forms a cytoplasmic vestibule. *Nature* **468**:585–588.

Wagner LE II, Groom LA, Dirksen RT, and Yule DI (2014) Characterization of ryanodine receptor type 1 single channel activity using "on-nucleus" patch clamp. *Cell Calcium* **56**:96–107.

Yamamoto T and Ikemoto N (2002) Spectroscopic monitoring of local conformational changes during the intramolecular domain-domain interaction of the ryanodine receptor. *Biochemistry* **41**:1492–1501.

Yan Z, Bai X, Yan C, Wu J, Li Z, Xie T, Peng W, Yin C, Li X, Scheres SHW, et al. (2015) Structure of the rabbit ryanodine receptor RyR1 at near-atomic resolution. *Nature* **517**:50–55.

Zalk R, Clarke OB, des Georges A, Grassucci RA, Reiken S, Mancia F, Hendrickson WA, Frank J, and Marks AR (2015) Structure of a mammalian ryanodine receptor. *Nature* **517**:44–49.

Zucchi R and Ronca-Testoni S (1997) The sarcoplasmic reticulum Ca^{2+} channel/ryanodine receptor: modulation by endogenous effectors, drugs and disease states. *Pharmacol Rev* **49**:1–51.

Address correspondence to: János Almássy, Department of Physiology, Faculty of Medicine, University of Debrecen, 4002 Debrecen, Hungary. E-mail: almassy.janos@med.unideb.hu; or Péter Pál Nánási, Department of Physiology, Faculty of Medicine, University of Debrecen, 4002 Debrecen, Hungary. E-mail: nanasi.peter@med.unideb.hu

MOLECULAR PHARMACOLOGY

Dantrolene requires Mg^{2+} and ATP to inhibit the ryanodine receptor

Gyula Diszházi, Zsuzsanna Édua Magyar, János András Mótyán, László Csernoch, István Jóna, Péter Pál Nánási, János Almássy

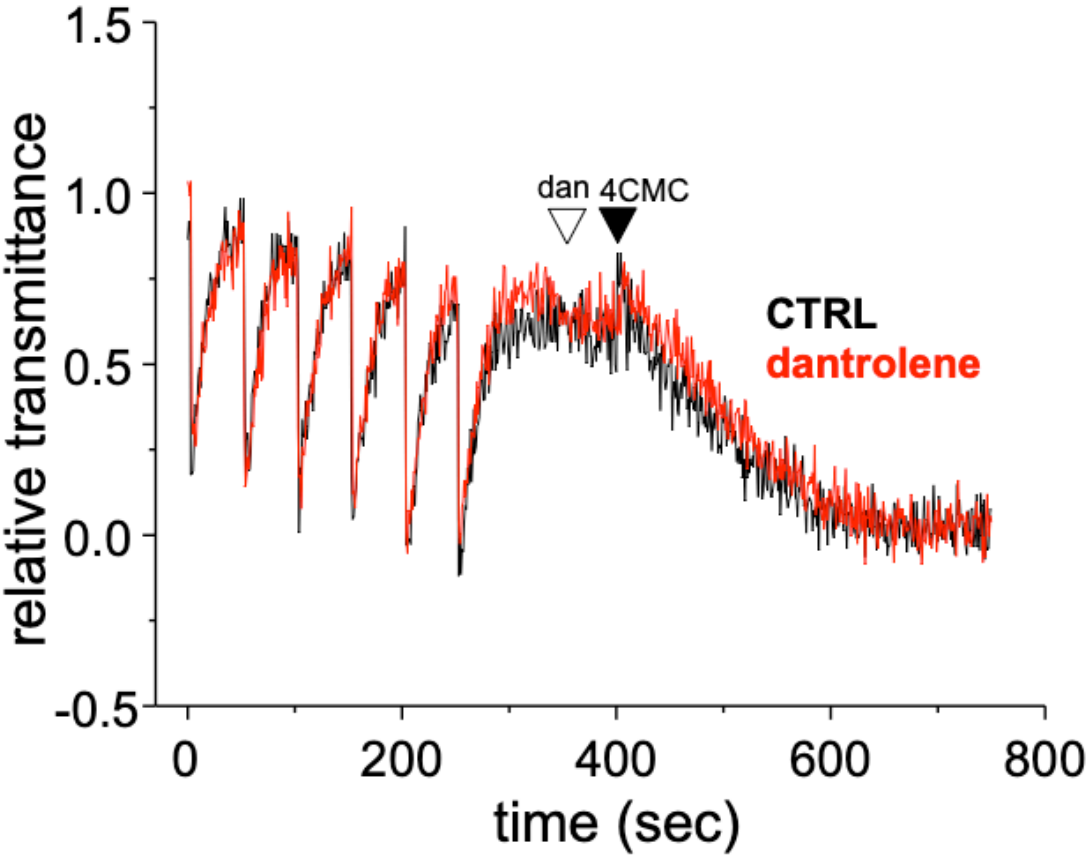

Supplementary Figure 1. Dantrolene is ineffective on cardiac sarcoplasmic reticulum vesicles.

Ca^{2+}-release from Ca^{2+}-loaded cardiac SR vesicles was triggered using 4CMC in the absence (control, black curve) or presence of dantrolene (red curve). Addition of dantrolene or DMSO is labeled with white- and the addition of 4CMC with black arrowheads.